ELSEVIER

www.elsevier.nl/locate/carres

Carbohydrate Research 329 (2000) 655–665

CARBOHYDRATE RESEARCH

X-ray structure determination and modeling of the cyclic tetrasaccharide *cyclo*-{→6)-α-D-Glc*p*-(1→3)-α-D-Glc*p*-(1→6)-α-D-Glc*p*-(1→3)-α-D-Glc*p*-(1→}

Gail M. Bradbrook [a], Katrin Gessler [a], Gregory L. Côté [b], Frank Momany [b], Peter Biely [c], Pierre Bordet [d], Serge Pérez [a], Anne Imberty [a,*]

[a] *CERMAV-CNRS (affiliated with Université Joseph Fourier), BP 53, F-38041 Grenoble, France*
[b] *Biopolymer Research Unit and Plant Polymer Unit, USDA, National Center for Agricultural Utilization Research, 1815 N. University Street, Peoria, IL 61604, USA*
[c] *Institute of Chemistry, Slovak Academy of Sciences, SK-842 38, Bratislava, Slovakia*
[d] *Laboratoire de Cristallographie, CNRS, BP 166, F-38042 Grenoble, France*

Received 25 May 2000; accepted 11 July 2000

Dedicated to the memory of Professor George A. Jeffrey.

Abstract

The cyclic tetrasaccharide *cyclo*-{→6)-α-D-Glc*p*-(1→3)-α-D-Glc*p*-(1→6)-α-D-Glc*p*-(1→3)-α-D-Glc*p*-(1→} is the major compound obtained by the action of endo-alternases on the alternan polysaccharide. Crystals of this cyclo-tetra-glucose belong to the orthorhombic space group $P2_12_12_1$ with $a = 7.620(5)$, $b = 12.450(5)$ and $c = 34.800(5)$ Å. The asymmetric unit contains one tetrasaccharide together with five water molecules. The tetrasaccharide adopts a plate-like overall shape with a very shallow depression on one side. The shape is not fully symmetrical and this is clearly apparent on comparing the (Φ, Ψ) torsion angles of the two α-(1→6) linkages. There is almost 10° differences in Φ and more than 20° differences in Ψ. The hydrogen bond network is asymmetric, with a single intramolecular hydrogen bond: O-2 of glucose ring 1 being the donor to O-2 of glucose ring 3. These two hydroxyl groups are located below the ring and their orientation, dictated by this hydrogen bond, makes the floor of the plate. Among the five water molecules, one located above the center of the plate occupies perfectly the shallow depression in the plate shape formed by the tetrasaccharide. Molecular dynamics simulation of the tetrasaccharide in explicit water allows rationalization of the discrepancies observed between the X-ray structures and data obtained previously by NMR.

Keywords: Cyclic-tetrasaccharide; Molecular modeling; Crystal structures; Alternan

1. Introduction

Interest in the polysaccharide alternan has increased within the past decade, due to its unusually low viscosity and relative resistance to microbial and enzymic degradation [1]. To

* Corresponding author. Tel.: +33-476-037603; fax: +33-476-547203.
E-mail address: imberty@cermav.cnrs.fr (A. Imberty).

0008-6215/00/$ - see front matter
PII: S0008-6215(00)00212-3

date, the only endo-alternanases reported [2,3] have yielded a cyclic tetrasaccharide as the major degradation product. This unique cyclic tetrasaccharide was shown to be *cyclo*-{→6)-α-D-Glc*p*-(1→3)-α-D-Glc*p*-(1→6)-α-D-Glc*p*-(1→3)-α-D-Glc*p*-(1→} (**1**) [4]. Initial difficulties in understanding the ^{13}C NMR spectrum of this compound led to a preliminary computer-generated molecular model of the structure, which helped explain the ^{13}C spectrum in terms of relatively unusual torsion angles about the C-3 linkages [4]. However, this model was not totally satisfactory, since the solution ^{13}C NMR spectrum exhibits only 12 resonances, indicating a symmetric molecule, whereas our preliminary modeling results suggested a significant degree of asymmetry.

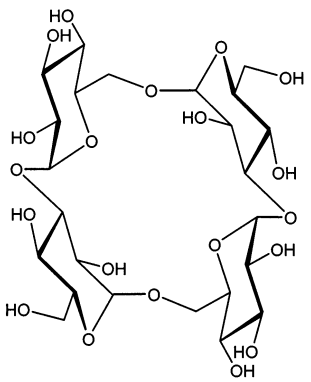

1

We have now succeeded in obtaining crystals of this compound suitable for X-ray diffraction, and report here the results of crystallographic analysis. Since our initial report, new computer modeling methods were applied to **1**, so that we are now able to present a comparison of molecular modeling and crystallographic studies of *cyclo*-{→6)-α-D-Glc*p*-(1→3)-α-D-Glc*p*-(1→6)-α-D-Glc*p*-(1→3)-α-D-Glc*p*-(1→}.

2. Results

Crystal structure.—Crystals of cyclo-tetra-glucose (**1**) belong to the orthorhombic space group $P2_12_12_1$ with $a = 7.620(5)$, $b = 12.450(5)$ and $c = 34.800(5)$ Å. The asymmetric unit contains one molecule of **1** together with five water molecules. Disorder is observed for one of the two hydroxymethyl groups, O(6)1, which can take two staggered orientations and for two of the water molecules, which can both occupy two closely related sites. The ORTEP representation of the cyclo-tetra-glucose (**1**) is represented in Fig. 1 together with the labeling of the atoms. The nomenclature used here gives the numbering of the atoms within the ring between parenthesis, followed by the numbering of the glucose ring. The positional and isotropic thermal parameters of the non-hydrogen atoms are given in Table 1. The atomic coordinates of the hydrogen atoms and the anisotropic temperature factors have been deposited together with bond lengths and bond angles. The estimated standard deviations range from 0.005 to 0.007 Å for the bond lengths and from 0.3 to 0.4° for the bond angles.

Conformations of the rings.—The C–C bond lengths of the glucose rings of **1** have a mean value of 1.52, which agrees with 1.527 Å, the mean value for carbohydrate rings [5]. The mean O-5–C-5 and C-1–O-5 bond lengths are also in agreement with the standard values. One of the distances between the anomeric carbon and glycosidic oxygen (C(1)3–O(6)4 at 1.38 Å) is shorter than usual for an α-linkage. All sugar rings are in the $^4C_1$ chair conformation with small variations being observed when the ring puckering is calculated using the Cremer and Pople parameters [6]. Puckering amplitudes of 0.589, 0.563, 0.582 and 0.546 Å and Θ angles of 5.9, 2.2, 4.6 and 2.5° are observed on going from glucose **1** to glucose **4**.

Conformations of the glycosidic linkages.—The valence and torsion angles of each of the glycosidic linkages are listed in Table 2. Both α-(1→6) linkages display valence angles close to 115.5°, whereas the α-(1→3) linkages have smaller valence angles with values centered around 113.7°. Both α-(1→6) linkages adopt a gauche–trans orientation for the ω torsion angle. The cyclic tetrasaccharide is not symmetrical and this is striking in comparison of the Φ and Ψ torsion angles of the two α-(1→6) linkages. They have almost 10° difference in Φ and more than 20° difference in Ψ. The orientations of the Φ and Ψ torsion angles of each linkage can be compared to the energy

maps previously computed with the MM3 program for the α-D-Glc*p*-(1→3)-α-D-Glc*p* (nigerose) [7] and α-D-Glc*p*-(1→6)-α-D-Glc*p* (isomaltose) [8] disaccharides. The conformations of the α-(1→3) linkages are close to the second energy minimum on the predicted energy surface, whereas the conformations of the α-(1→6) linkages are situated between two minima of the energy surface, on a conformational transition path located about 3 kcal/mol above the global minimum.

Overall shape of the tetrasaccharide.—The tetrasaccharide adopts a plate-like overall shape with a very shallow depression on one face. On defining a plane passing through the four glycosidic oxygen atoms, the molecule exhibits limited deviations below and above this plane. For the 24 atoms of the six-membered rings, the RMS deviations of the height on each side of this plane is less than 0.8 Å, the maximum deviations being observed for the carbons at position 2. These C-2 carbons of rings 1 and 3 are below the plane (by 1.05 and 1.20 Å, respectively), while the C-2 carbons of rings 2 and 4 are above this plane (by 1.42 and 1.20 Å, respectively). Pendant hydroxyl groups at position 2 and 4 point away from either of the plate faces. As illustrated by the description of the rings, the glycosidic linkages and the deviations from plane, the tetrasaccharide is not perfectly symmetrical. When analyzing the hydrogen bond network, it appears that its symmetry is indeed broken by an intramolecular hydrogen bond in which O-2 of glucose ring 1 donates its hydrogen to O-2 of glucose ring 3. These two hydroxyl groups are located below the ring with their resulting orientation producing the floor of the plate. No other intramolecular hydrogen bonds are observed in the tetrasaccharide, a situation very different from cyclodextrins in which neighbouring glucose residues interact

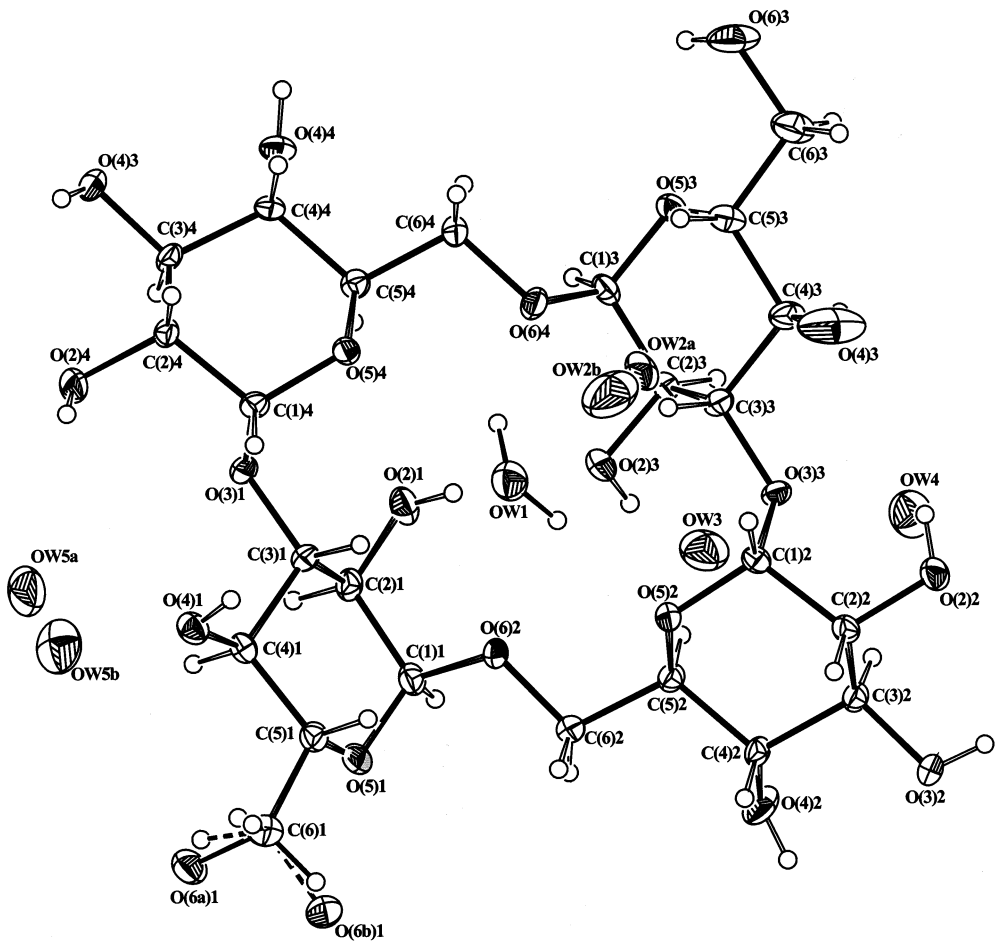

Fig. 1. ORTEP view of the cyclic tetrasaccharide **1** along with the labelling of the atoms. Thermal ellipsoids are drawn at the 30% probability level.

Table 1
Final fractional coordinates and equivalent isotropic thermal parameters for the non hydrogen atoms of **1**

Atom (occupancy) [a]	x/a	y/b	z/c	U_{iso} (Å^2)
C(1)1	−0.2660(6)	0.3403(3)	0.54346(12)	0.041(2)
C(2)1	−0.1282(6)	0.4132(3)	0.56170(12)	0.029(2)
C(3)1	−0.2106(5)	0.4762(3)	0.59412(12)	0.022(2)
C(4)1	−0.3678(5)	0.5399(3)	0.57785(11)	0.029(2)
C(5)1	−0.4987(6)	0.4595(3)	0.56131(11)	0.032(2)
C(6)1	−0.6613(6)	0.5093(4)	0.54471(14)	0.036(3)
O(2)1	0.0234(4)	0.3546(2)	0.57267(10)	0.0294(16)
O(3)1	−0.0831(4)	0.54708(19)	0.61125(7)	0.0225(14)
O(4)1	−0.4456(4)	0.6078(2)	0.60507(8)	0.0360(17)
O(5)1	−0.4160(4)	0.3983(2)	0.53133(8)	0.0448(18)
O(6a)1 (74%)	−0.6325(6)	0.5782(3)	0.51461(13)	0.040(3)
O(6b)1 (26%)	−0.7491(16)	0.4376(9)	0.5221(4)	0.030(7)
C(1)2	−0.3497(5)	0.0101(3)	0.64388(12)	0.0188(19)
C(2)2	−0.4568(5)	−0.0892(3)	0.63375(11)	0.019(2)
C(3)2	−0.4384(5)	−0.1176(3)	0.59152(12)	0.023(2)
C(4)2	−0.4810(5)	−0.0203(3)	0.56682(11)	0.028(2)
C(5)2	−0.3707(6)	0.0756(3)	0.57925(11)	0.023(2)
C(6)2	−0.4218(6)	0.1772(3)	0.55814(13)	0.035(2)
O(2)2	−0.4137(4)	−0.1775(2)	0.65803(8)	0.0321(16)
O(3)2	−0.5561(4)	−0.2014(2)	0.58104(9)	0.0449(19)
O(4)2	−0.4408(5)	−0.0409(2)	0.52740(9)	0.067(2)
O(5)2	−0.3979(4)	0.09630(19)	0.61956(8)	0.0259(15)
O(6)2	−0.3085(4)	0.2617(2)	0.57127(8)	0.0402(17)
C(1)3	0.2087(6)	0.1665(3)	0.65898(12)	0.022(2)
C(2)3	0.0898(5)	0.0946(3)	0.63524(11)	0.022(2)
C(3)3	−0.0537(5)	0.0515(3)	0.66162(11)	0.022(2)
C(4)3	0.0282(6)	−0.0109(4)	0.69393(12)	0.025(2)
C(5)3	0.1579(6)	0.0600(4)	0.71562(12)	0.024(2)
C(6)3	0.2660(7)	−0.0019(5)	0.74453(15)	0.040(3)
O(2)3	0.0221(5)	0.1533(2)	0.60400(9)	0.0478(19)
O(3)3	−0.1719(3)	−0.0172(2)	0.64032(8)	0.0188(14)
O(4)3	−0.1025(6)	−0.0455(5)	0.72041(11)	0.066(3)
O(5)3	0.2848(4)	0.1066(2)	0.68973(8)	0.0208(14)
O(6)3	0.3697(5)	0.0700(3)	0.76760(10)	0.052(2)
C(1)4	−0.0969(5)	0.5522(3)	0.65142(11)	0.0171(19)
C(2)4	−0.0043(5)	0.6524(3)	0.66661(12)	0.023(2)
C(3)4	0.1932(5)	0.6430(3)	0.66268(12)	0.022(2)
C(4)4	0.2575(5)	0.5396(3)	0.67963(11)	0.0173(19)
C(5)4	0.1569(5)	0.4424(3)	0.66412(12)	0.025(2)
C(6)4	0.2060(6)	0.3424(3)	0.68627(15)	0.034(2)
O(2)4	−0.0670(4)	0.7471(2)	0.64791(10)	0.0304(16)
O(3)4	0.2740(4)	0.7328(2)	0.68151(9)	0.0322(16)
O(4)4	0.4387(4)	0.5233(2)	0.67099(8)	0.0201(14)
O(5)4	−0.0292(4)	0.4588(2)	0.66965(8)	0.0178(14)
O(6)4	0.1091(4)	0.2522(2)	0.67155(10)	0.0243(15)
Ow1	−0.3074(6)	0.2866(3)	0.66828(12)	0.045(2)
Ow2a (44%)	−0.326(3)	0.173(2)	0.7398(5)	0.052(10)
Ow2b (56%)	−0.381(12)	0.208(6)	0.7382(6)	0.16(3)
Ow3	0.0815(6)	0.0165(3)	0.54636(11)	0.077(3)
Ow4	0.0777(6)	−0.1959(3)	0.57590(12)	0.058(2)
Ow5a (35%)	0.045(3)	0.7367(10)	0.5044(4)	0.13(2)
Ow5b (65%)	−0.1067(16)	0.7069(6)	0.5101(2)	0.103(9)

[a] Occupancy is given in parentheses when different from 100%.

along the outer edge of the cycle via their hydroxyls at position 2 and 3 (see review [9]).

Hydration scheme.—Five water molecules are co-crystallized with compound **1** and are displayed in the ORTEP diagram of Fig. 1. Two of the five water molecules are disordered and each resides on two nearby equally probable positions. Among the five water molecules, the first one (OW1) has a key position above the center of the plate. Its hydrogen atoms were clearly located by Fourier difference and they are within hydrogen bonding distance from two intra-ring oxygen atoms, O(5)2 and O(5)4. This water makes two three-centered hydrogen bonds since each of its hydrogen atoms is also involved in a weaker bond ($d_{O\cdots O}$ about 3.3 Å) with the two glycosidic oxygens of the α-(1→6) linkages. When calculating the Connolly surface of the tetrasaccharide (Fig. 2), this water molecule neatly occupies the shallow depression on the plate shape. Its two hydrogen atoms point toward a region with negative electrostatic potential created by a cluster of slightly negatively charged acetal oxygen atoms.

All other water molecules are also connected by numerous hydrogen bonds to the carbohydrate and/or to other waters. Fig. 3 displays the complete hydrogen bond network and a detailed description is given in Table 3. Each tetrasaccharide is involved in one intramolecular hydrogen bond, nine hydrogen bonds with neighbouring cyclic oligosaccharides and 11 hydrogen bonds with water molecules. This results in an average of more than five hydrogen bonds per glucose unit.

Packing.—The mode of molecular packing has been analyzed by applying the atom-pair procedure of Kitaigorodsky [10]. For a reference molecule, all contacts with the surrounding molecules are explored. In this approach, the energy of interaction can be calculated using a 6-exp potential with the coefficients proposed by Fillipini and Gavezzoti [11]. From this analysis, the van der Waals interactions along the *a* axis are twice as much as for the other axes. Furthermore, translation along *a* is stabilized by an intermolecular O(4)1···O(4)4 hydrogen bond. The translation operation along *b* has the second most favorable van der Waals interaction energy and stabilization along this axis arises from intermolecular hydrogen bonds (Table 3). Two projections of the packing mode are given in Fig. 4.

Modeling.—Several molecular dynamics simulation were performed with the inclusion of explicit water molecules. No large conformational change was observed during these simulations and it can be hypothesized that

Table 2
Valence and torsion angles (°) at the glycosidic linkages of **1**

Angle		Angle	
α-(1→6) linkage			
O(5)1–C(1)1–O(6)2	111.8(3)	O(5)3–C(1)3–O(6)4	112.9(3)
C(1)1–O(6)2–C(6)2	115.3(3)	C(1)3–O(6)4–C(6)4	115.7(3)
O(6)2–C(6)2–C(5)2	107.7(3)	O(6)4–C(6)4–C(5)4	110.7(5)
α-(1→3) linkage			
O(3)3–C(1)2–O(5)2	112.4(3)	O(3)1–C(1)4–O(5)4	112.3(3)
C(1)2–O(3)3–C(3)3	114.4(3)	C(1)4–O(3)1–C(3)1	112.9(3)
O(3)3–C(3)3–C(2)3	110.2(3)	O(3)1–C(3)1–C(2)1	110.3(3)
Dihedral angle		Dihedral angle	
α-(1→6) linkage			
(*Φ*) O(5)1–C(1)1–O(6)2–C(6)2	64.2(4)	O(5)3–C(1)3–O(6)4–C(6)4	73.4(4)
(*Ψ*) C(1)1–O(6)2–C(6)2–C(5)2	146.9(3)	C(1)3–O(6)4–C(6)4–C(5)4	123.3(4)
(*ω*) O(6)2–C(6)2–C(5)2–O(5)2	61.1(4)	O(6)3–C(6)3–C(5)3–O(5)3	60.5(4)
α-(1→3) linkage			
(*Φ*) O(5)2–C(1)2–O(3)3–C(3)3	80.6(4)	O(5)4–C(1)4–O(3)1–C(3)1	75.1(4)
(*Ψ*) C(1)2–O(3)3–C(3)3–C(4)3	112.0(4)	C(1)4–O(3)1–C(3)1–C(4)1	99.6(4)
C(1)2–O(3)3–C(3)3–C(2)3	−127.3(3)	C(1)4–O(3)1–C(3)1–C(2)1	−140.2(3)

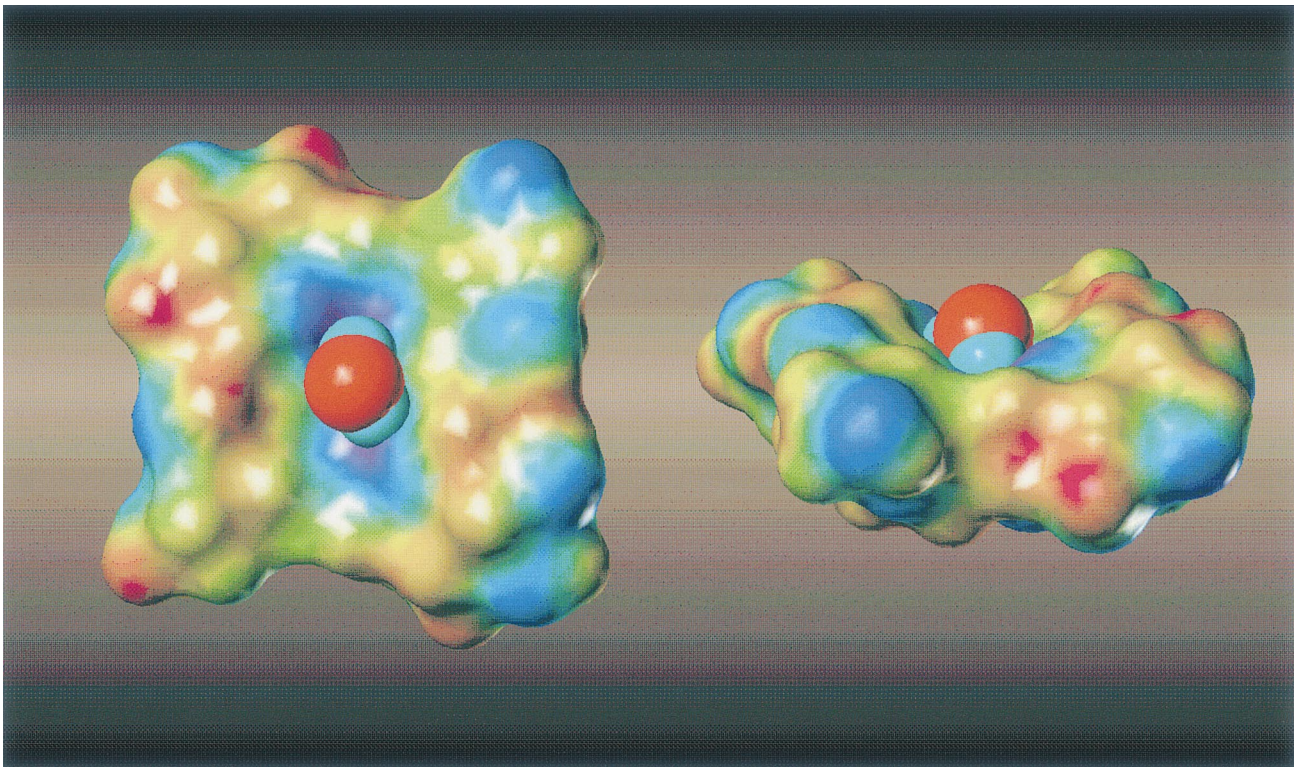

Fig. 2. Conolly surface of the cyclic tetrasaccharide **1** color coded following the electrostatic potential (blue for negative charges to red for positive charges). Only one water molecule has been displayed using a CPK representation.

macroring cyclization constraints limit the flexibility of each linkage. The average values of the torsion angles at the α-(1→3) linkage are 90 and 95° for Φ and Ψ, respectively, with variations in the range of $\pm 20°$. The (Φ, Ψ, ω) torsion angles at the α-(1→6) linkage have average values of about (60°, 175°, 55°) with variation ranges similar to the other linkage, except for the Φ angle that is slightly more flexible and can vary in a 60° window. Much more flexibility is observed for the hydroxyl groups, and the life time of any hydrogen bond does not exceed a few ps tens.

All the simulations converged to one low energy conformation (Fig. 5). In this model, the α-(1→6) linkages displays Φ and Ψ values centered around 77 and 106°, respectively, in good agreement with the low energy region of the nigerose disaccharide, as calculated with the MM3 program [7]. The α-(1→6) linkages adopt a gauche–trans orientation for the ω torsion angles and the (Φ, Ψ) values correspond to the lowest energy ones as calculated for the isomaltose disaccharide [8]. The resulting molecule is almost symmetrical in shape since the maximal deviations between equivalent torsion angles is of only 10°.

The solution model has close similarities with the crystal structure, and superimposing all non-hydrogen atoms (Fig. 5) yielded a rms of 0.51 Å. Both molecules have a plate shape, with O-2 of ring 1 and 3 forming the floor of the plate. In both cases, the gauche–trans orientations of the α-(1→6) linkages give an extended shape to this linkage. However, on closer inspection, there are significant differences between the experimental X-ray structure and the calculated solution structure. The crystal structure appears to be more flat and less symmetrical than the solution model. The main differences are found in the torsion angles across the bridging methoxy groups. In particular, the C-5–C-6–O-6–C-1 torsion angles are both close to the extended trans ($\sim 180°$) form in the calculated model, whereas these torsion angles are particularly puckered in the X-ray structure (147 and 123°). The asymmetry we see in the bridging methoxy groups occurs, as well in the ϕ_H and ϕ_H dihedral angles where ψ_H is $\sim 40°$ on both

sides, but ψ_H varies from -8 to $-20°$. The asymmetry in torsion angles is nearly missing in the solution structures, although some residual asymmetry exists because of the interresidue 2-hydroxy interactions. During the dynamics simulation, the 2-hydroxy groups or rings 1 and 3 change interaction configuration by flipping the 2-hydroxy hydrogen atom on one side either toward or away from the 2-hydroxy oxygen across the ring. By freezing this equilibrium we tend to create a distortion in the tetrasaccharide structure, as shown in Fig. 5. Although this is not a high energy distortion, it shows up in the energy minimized structure as deviations from symmetry.

In order to analyze the driving forces in the conformational difference observed between the crystal structure conformation and the theoretical one, the tetrasaccharide conformation observed in the solid state was allowed to optimize, either in the presence or in the absence of the bridging water molecule. In both cases, conformation converged to the one predicted from the modeling study above, characterized by a much less planar shape. It could then be concluded that packing energy gives the energy needed for the distortion in the Ψ angle at the α-(1→6) linkage, resulting in the peculiar flat shape observed here. To assess the energy associated with attaining the crystal structure, we have applied dihedral angle torsion forces to the C-6–O-6 bonds to bring them to the X-ray structure values. The energy required to do this and obtain a conformation

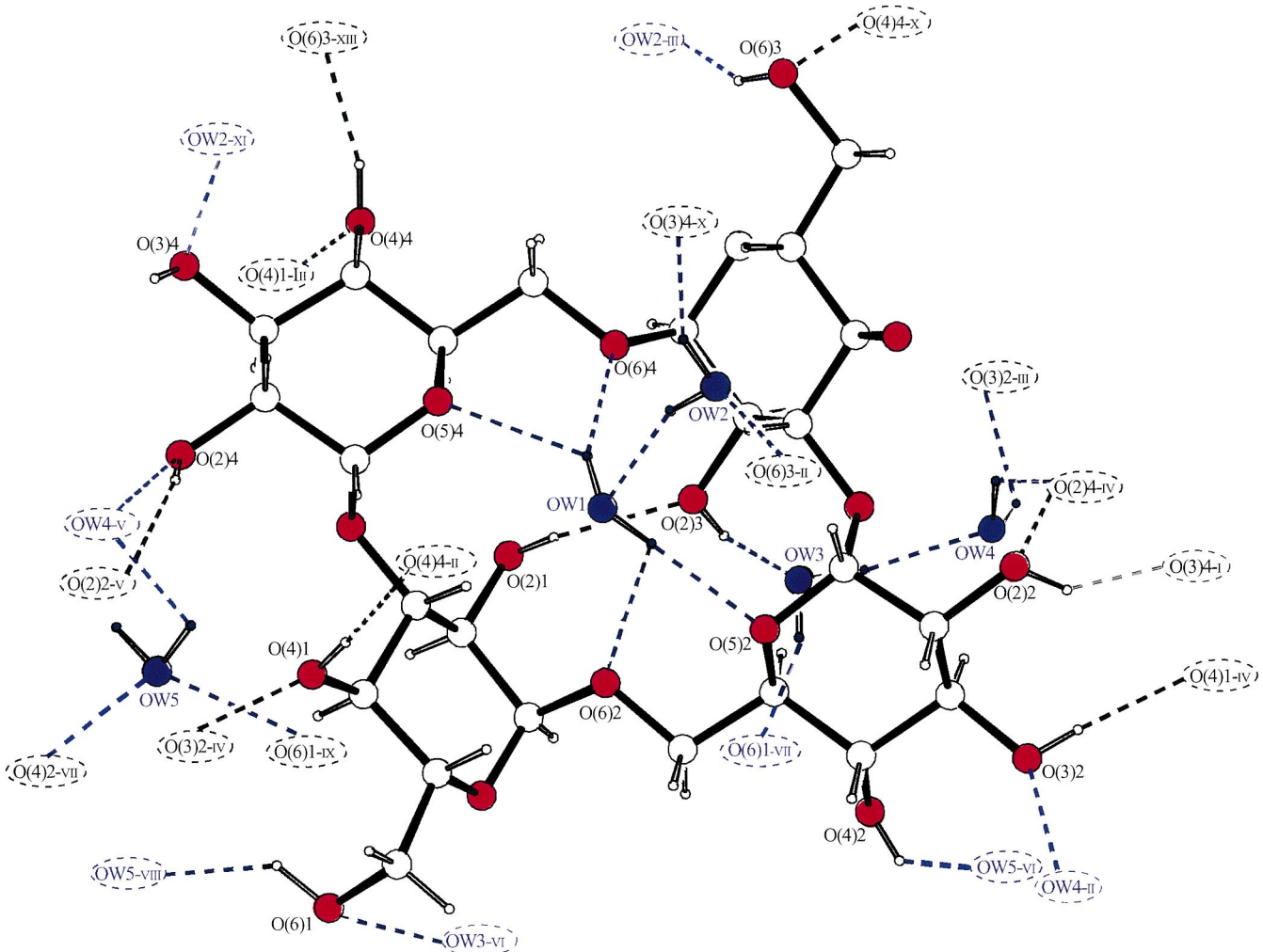

Fig. 3. Complete hydrogen bond networks in the crystal structure of the cyclic tetrasaccharide **1**. Carbohydrate and water oxygen atoms have been colored in blue and red, respectively. The neighboring atoms have been given a code to indicate the symmetry involved: (I) $x-1, y-1, z$; (II) $x-1, y, z$; (III) $x+1, y, z$; (IV) $x, y-1, z$; (V) $x, y+1, z$; (VI) $x-1/2, -y+1/2, -z+1$; (VII) $x+1/2, -y+1/2, -z+1$; (VIII) $x-1/2, -y+3/2, -z+1$; (IX) $x+1/2, -y+3/2, -z+1$; (X) $-x, y-1/2, -z+3/2$; (XI) $-x, y+1/2, z+3/2$; (XII) $-x+1, y-1/2, -z+3/2$; (XIII) $-x+1, y+1/2, z+3/2$.

Table 3
Hydrogen bonds [a]

Hydrogen bond donor	Hydrogen bond acceptor	Symmetry operation on acceptor	$d_{O\cdots O}$ (Å)	$d_{H\cdots O}$ (Å)	$\Theta_{O-H\cdots O}$ (°)
O(2)1	O(2)3	x, y, z (intra)	2.74	1.93	141
O(4)1	O(4)4	$x-1, y, z$	2.67	1.77	156
O(6)1 [b]	Ow5	$x-1/2, -y+3/2, -z+1$	2.75	2.02	134
O(2)2 [b]	O(3)4	$x-1, y-1, z$	2.75	1.83	164
O(3)2	O(4)1	$x, y-1, z$	2.66	1.71	176
O(4)2	O5w	$x-1/2, -y+1/2, -z+1$	2.68	2.21	110
O(2)3	O3w	x, y, z	2.67	1.77	161
O(6)3	O2w	$x+1, y, z$	2.83	2.06	137
O(2)4	O(2)2	$x,y+1,z$	2.82	1.91	162
O(4)4	O(6)3	$-x+1, y+1/2, -z+3/2$	2.66	1.73	166
Ow1	O(5)2	x, y, z	2.99	2.06	168
Ow1	O(5)4	x, y, z	3.01	2.34	128
Ow1	O(6)2	x, y, z	3.39	2.77	124
Ow1	O(6)4	x, y, z	3.00	2.30	158
Ow2 [b]	O(3)4	$-x, y-1/2, -z+3/2$	2.87	1.99	154
Ow2 [b]	Ow1	x, y, z	2.84	1.95	156
Ow3 [b]	O(6)1	$x+1/2, -y+1/2, -z+1$	2.92	2.37	117
Ow3 [b]	Ow4	x, y, z	2.84	2.01	145
Ow4 [b]	O(3)2	$x+1, y, z$	2.80	1.98	143
Ow4 [b]	O(2)4	$x, y-1, z$	2.83	2.03	140
Ow5 [b]	Ow4	$x, y+1, z$	2.64	2.06	118

[a] All of the hydrogen atoms were corrected for the distance of the O–H distances (0.95 Å). The hydroxyl groups that could not be located on the difference maps have been modeled according to the hydrogen bond network.

[b] The location of the corresponding hydrogen atom has not been calculated from the Fourier difference map but deduced from the hydrogen bonding network.

very close to the X-ray conformer is ~ 8.5 kcal/mol. This is a small energy penalty to pay for such large changes in structure, and it can be easily provided by packing forces. These calculations indicate that the solution conformation may indeed be more symmetric than the crystal structure. These results agree with results from NMR analysis [4]. It should also be noted that NMR measurements provide time-averaged conformational information. The existence of slightly asymmetric shapes with fast interconversion, resulting from a hydrogen bond flip, would be in agreement with the observed spectra.

3. Discussion and conclusions

Aside from the basic scientific interest in understanding the structure of this unique tetrasaccharide, there may also be practical implications. Cyclic inulin oligosaccharides have been shown to bind to various metallic cations in aqueous solution. The cyclic inulin hexasaccharide [12] and its methyl derivative [13] have been co-crystallized with barium cation. Interestingly, a molecular modeling study on inulin oligosaccharides predicted a disk shape for the rings composed of six to eight fructofuranose units and calculation of molecular electrostatic potential demonstrated the existence of a negatively charged face [14]. Therefore, the crystal structure of the compound studied here shares some structural features with the cyclic inulo-oligosaccharides in that there is a concentration of slightly negatively charged acetal oxygen atoms in the center of the cavity. Our cyclic tetrasaccharide compound has been patented [15], and certain derivatives are currently being investigated for their potential use as therapeutic and diagnostic agents. A better idea of its three-dimensional structure may be helpful in targeting some of these derivatives for specific applications.

4. Experimental

Materials.—The cyclic tetrasaccharide was prepared by enzymic degradation of alternan and isolated by high-performance liquid chromatography (HPLC), as previously described [4]. Microcrystals were obtained from satd MeOH solns. Crystals suitable for X-ray analysis were grown by the sitting drop method from a solution containing 20% poly(ethylene glycol) 400. Seeding of the drop with ground up microcrystalline sample proved to be the key step in obtaining crystals.

Crystal structure determination.—Data were collected from a single crystal mounted on a glass fiber using a KappaCCD Nonius diffractometer equipped with monochromatized Ag K_α radiation. Diffraction patterns were recorded by the oscillation technique using a CCD detector and were processed with DENZO-SMN and SCALEPACK [16]. All the intensities were corrected for background contribution. Lorentz and polarization corrections were applied, but no correction was made for absorption, given the crystal dimensions and the wavelength used. Scattering factors were taken from the International Table of Crystallography. The crystal structure was solved and refined by SHELX-97 [17], using full-matrix least-squares on F^2. Real space refinement was performed using Xtalview [18]. A summary of crystallographic data, data collection and structure refinement is presented in Table 4.

Computational modeling methods.—Modeling simulations were carried out using the force field denoted AMB99C [19,20], implemented in the Molecular Simulations Inc., San Diego, CA(MSI) InsightII/4.0 Discover programs. Energy calculations used a dielectric constant of unity with the electrostatic and non-bonded van der Waals 1–4 terms scaled by 0.5. Partial atomic charges were the same as described previously [19,20] for carbohydrates. Empirical energy minimization was carried out to a gradient of less than ~ 0.001 kcal/mol, and molecular dynamics simulations were performed using the MSI Discover program. Calculations were carried out at 300 K,

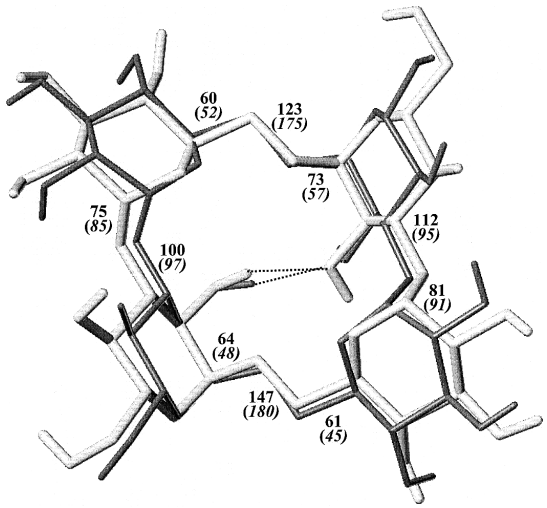

Fig. 5. Superimposition of the structures together with values of selected torsion angles for **1** as seen by X-ray (thick sticks and normal police) and modeling (thin dark sticks and italic police). For the sake of clarity, only hydrogen atoms linked to oxygen were displayed.

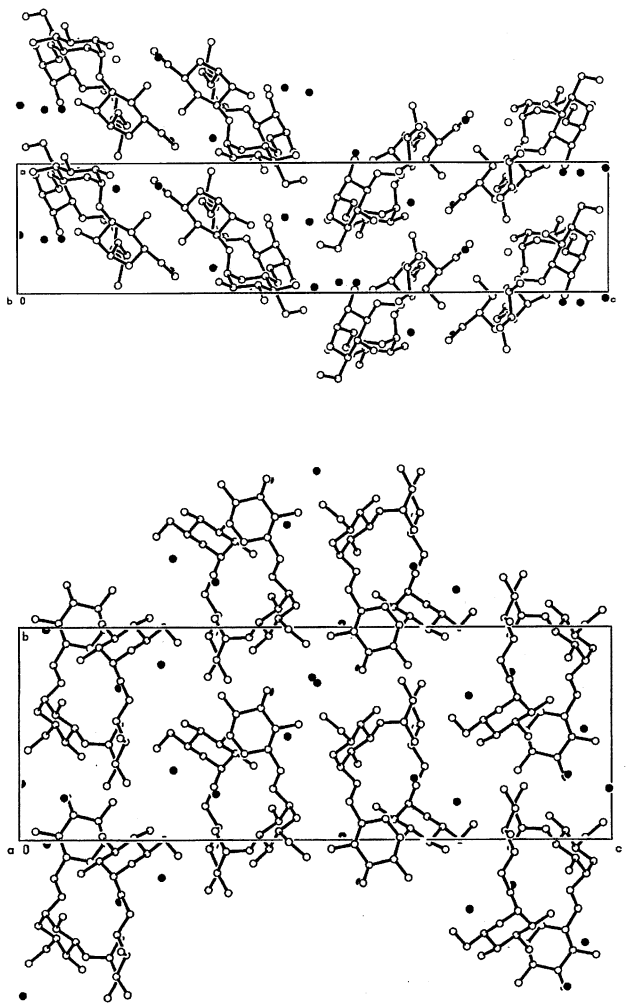

Fig. 4. Two different views of the packing arrangement of the cyclic tetrasaccharide **1**. Water molecules are displayed as dark dots. Hydrogen atoms have been omitted for clarity.

with the temperature controlled by a weak coupling to a temperature bath. Time steps of 1 fs were used to calculate velocities, but results were stored for examination at picosecond (ps) intervals. The equilibration time was approximately 1/10 of the total simulation time. Explicit hydrogen atoms are included in all calculations and both heavy atoms and hydrogen atoms are allowed to move on all molecules.

TIP3P water potentials were used throughout all simulations without internal constraints. A box with periodic boundaries was created to allow application of image conditions and the molecule was placed in the box (example box dimensions, $13.9 \times 13.9 \times 9.3$ Å). Water molecules were added to the box around the molecule, and energy minimization and short dynamics steps carried out. After each simulation we attempted to add more water molecules to fill void spaces. The explicit image model with cutoff distances of 12 Å and a switching function with a buffer width of 2 Å was used for water boxes. This method did not require that the cutoffs be less than half of the shortest unit cell length. The pressure in the box was monitored at the end of the equilibrium stage of dynamics and some simulations were made running under constant pressure (PNT) conditions. This allows the cell to expand or contract with the energy. Results from a 100 ps PVT simulation are described. A starting conformation for the cyclic tetrasaccharide was obtained using a combination of dynamics simulations at elevated temperatures (~ 600 K) and structural preferences for allowed conformational space. Few combinations of bridging dihedral angles allowed ring closure at low energy and these combinations were examined more carefully. The resulting conformation shown in Fig. 5 resulted from several different dynamics simulations, some in which the starting conformation was considerably distorted from the symmetric form.

Table 4
Crystallographic data and structure refinement

Crystal color and shape	colorless plates
Empirical formula	$C_{24}H_{40}O_{20}\cdot 5H_2O$
Formula weight	738.26
Crystal size (mm)	$0.2 \times 0.2 \times 0.02$
Temperature (K)	298
Wavelength (Ag K_α) (Å)	0.5608
Crystal system	orthorhombic
Space group	$P2_12_12_1$
Unit cell dimensions	
a (Å)	7.620(5)
b (Å)	12.450(5)
c (Å)	34.800(5)
V (Å^3)	3301.6(3)
Z	4
D_{calc} (g cm^{-3})	1.416
$F(000)$	1520.0
2θ Range (°)	3–42
Index ranges	h: 0–9, k: 0–14, l:0–38
No. unique reflections	3387
No. observed ($I > 2\sigma(I)$) reflections	3019 ($R_{sym} = 0.047$)
Completeness 0.89 − 0.75 Å (%)	70.4
Completeness 0.94 − 0.89 Å (%)	91.6
Overall completeness to 0.89 Å (%)	97
Data/restraints/parameters	3387/6/491
Goodness-of-fit on F^2	1.220
Final R	0.0506
Final wR	0.0515

5. Miscellaneous

Geometrical calculations, and ORTEP illustrations of the crystal structure were obtained with PLATON [21]. Accessible surface calculations were performed using the MOLCAD program [22].

6. Supplementary material

Crystallographic data (excluding structure factors) for the structure in this paper have been deposited with the Cambridge Crystallographic Data Centre as supplementary publication nos. CCDC 146356. Copies of the data may be obtained free of charge from: The Director, CCDC, 12 Union Road, Cambridge, CB2 1EZ, UK (fax: +44-1223-336033; e-mail: deposit@ccdc.cam.ac.uk or www: http://www.ccdc.cam.ac.uk).

Acknowledgements

The authors thank Dr Al French for his helpful discussions and for providing the pre-

liminary computer-generated model which provided the incentive for this study. We are also grateful to Catherine Gautier for excellent technical assistance. G.M.B. is supported by a Grant Fellowship from CARENET-2 (EU network no. ERB FMRX CT96 0025) and K.G. benefits from a Marie Curie Training Grant Fellowship (no. BIO4-98-5037).

References

[1] G.L. Côté, T.D. Leathers, J.A. Ahlgren, H.A. Wyckoff, G.T. Hayman, P. Biely, in H. Okai, O. Mills, A.M. Spanier, M. Tamura (Eds.), *Chemistry of Novel Foods*, American Chemical Society, Washington DC, 1997.
[2] P. Biely, G.L. Côté, A. Burgess-Cassler, *Eur. J. Biochem.*, 226 (1994) 633–639.
[3] H.A. Wyckoff, G.L. Côté, P. Biely, *Curr. Microbiol.*, 32 (1996) 343–348.
[4] G.L. Côté, P. Biely, *Eur. J. Biochem.*, 226 (1994) 641–648.
[5] G.A. Jeffrey, R. Taylor, *J. Comput. Chem.*, 1 (1980) 99–109.
[6] D. Cremer, J.A. Pople, *J. Am. Chem. Soc.*, 97 (1975) 1354–1358.
[7] M.K. Dowd, J. Zeng, A.D. French, P.J. Reilly, *Carbohydr. Res.*, 230 (1992) 233–244.
[8] M.K. Dowd, P.J. Reilly, A.D. French, *Biopolymers*, 34 (1994) 625–638.
[9] W. Saenger, J. Jacob, K. Gessler, T. Steiner, D. Hoffmann, H. Sanbe, K. Koizumi, S.M. Smith, T. Takaha, *Chem. Rev.*, 98 (1998) 1787–1802.
[10] A.I. Kitaigorodsky, *Molecular Crystals and Molecules*, Academic, New York, 1973.
[11] G. Fillipini, A. Gavezzoti, *Acta Crystallogr., Sect. B*, 49 (1993) 868–880.
[12] M. Sawada, T. Tanaka, Y. Takai, T. Hanafusa, T. Taniguchi, M. Kawamura, T. Uchiyama, *Carbohydr. Res.*, 217 (1991) 7–17.
[13] Y. Takai, Y. Okumura, T. Tanaka, M. Sawada, S. Takahashi, M. Shiro, M. Kawamura, T. Uchiyama, *J. Org. Chem.*, 59 (1994) 2967–2975.
[14] S. Immel, G.E. Schmitt, F.W. Lichtenthaler, *Carbohydr. Res.*, 313 (1998) 91–105.
[15] G.L. Côté, P. Biely, US Patent 5,889,179 (1999).
[16] Z. Otwinowski, W. Minor, *Methods Enzymol.*, 276 (1997) 307–326.
[17] G.M. Sheldrick, SHELX-97, Program for Crystal Structure Refinement, University of Göttingen, Germany, 1997.
[18] D.E. McRee, *J. Mol. Graph.*, 10 (1992) 44–46.
[19] F.A. Momany, J.L. Willett, *Carbohydr. Res.*, 326 (2000) 194–209.
[20] F.A. Momany, J.L. Willett, *Carbohydr. Res.*, 326 (2000) 210–226.
[21] A.L. Spek, *J. Appl. Crystallogr.*, 21 (1988) 578.
[22] M. Waldherr-Teschner, T. Goetze, W. Heiden, M. Knoblauch, H. Vollhardt, J. Brickmann, in F.H. Post, A.J.S. Hin (Eds.), *Advances in Scientific Visualization*, Springer, Heidelberg, 1992.